

QC  
801  
.U651  
no. 58  
c.2  
U.S. GOVERNMENT  
PUBLICATION

CPM X  
101

NOAA TR NOS 58

# NOAA Technical Report NOS 58

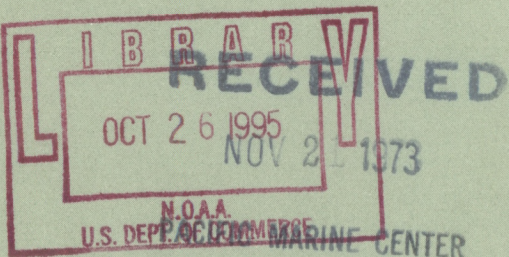
U.S. DEPARTMENT OF COMMERCE  
National Oceanic and Atmospheric Administration  
National Ocean Survey



## Telemetering Hydrographic Tide Gauge

CHARLES W. ISELEY

ROCKVILLE, MD.  
July 1973





## NOAA TECHNICAL REPORTS National Ocean Survey Series

The National Ocean Survey (NOS) provides charts and related information for the safe navigation of marine and air commerce. The survey also furnishes other earth science data—from geodetic, hydrographic, oceanographic, geomagnetic, seismologic, gravimetric, and astronomic surveys, observations, investigations, and measurements—to protect life and property and to meet the needs of engineering, scientific, defense, commercial, and industrial interests.

Because many of these reports deal with new practices and techniques, the views expressed are those of the authors and do not necessarily represent final survey policy. NOS series NOAA Technical Reports is a continuation of, and retains the consecutive numbering sequence of, the former series, Environmental Science Services Administration (ESSA) Technical Reports Coast and Geodetic Survey (C&GS), and the earlier series, C&GS Technical Bulletins.

Those publications marked by an asterisk are out of print. The others are available through the Superintendent of Documents, U.S. Government Printing Office, Washington, D.C. 20402. Price as indicated. Beginning with 39, microfiche is available at the National Technical Information Service (NTIS), U.S. Department of Commerce, Sills Bldg., 5285 Port Royal Road, Springfield, Va. 22151. Price \$0.95. Order by accession number, when given, in parentheses.

### COAST AND GEODETIC SURVEY TECHNICAL BULLETINS

- \*No. 22 Tidal Current Surveys by Photogrammetric Methods. Morton Keller, October 1963.
- \*No. 23 Aerotriangulation Strip Adjustment. M. Keller and G. C. Tewinkel, August 1964.
- \*No. 24 Satellite Triangulation in the Coast and Geodetic Survey, February 1965.
- \*No. 25 Aerotriangulation: Image Coordinate Refinement. M. Keller and G. C. Tewinkel, March 1965.
- \*No. 26 Instrumented Telemetering Deep Sea Buoys. H. W. Straub, J. M. Arthaber, A. L. Copeland, and D. T. Theodore, June 1965.
- \*No. 27 Survey of the Boundary Between Arizona and California. Lansing G. Simmons, August 1965.
- \*No. 28 Marine Geology of the Northeastern Gulf of Maine. R. J. Malloy and R. N. Harbison, February 1966.
- \*No. 29 Three-Photo Aerotriangulation. M. Keller and G. C. Tewinkel, February 1966.
- \*No. 30 Cable Length Determinations for Deep-Sea Oceanographic Operations. Robert C. Darling, June 1966.
- \*No. 31 The Automatic Standard Magnetic Observatory. L. R. Alldredge and I. Saldukas, June 1966.

### ESSA TECHNICAL REPORTS

- \*C&GS 32 Space Resection in Photogrammetry. M. Keller and G. C. Tewinkel, September 1966.
- \*C&GS 33 The Tsunami of March 28, 1964, as Recorded at Tide Stations, M. G. Spaeth and S. C. Berkman, July 1967.
- \*C&GS 34 Aerotriangulation: Transformation of Surveying and Mapping Coordinate Systems. Melvin J. Umbach, August 1967.
- \*C&GS 35 Block Analytic Aerotriangulation. M. Keller and G. C. Tewinkel, November 1967.
- \*C&GS 36 Geodetic and Grid Angles—State Coordinate Systems. Lansing G. Simmons, January 1968.
- \*C&GS 37 Precise Echo Sounding in Deep Water. George A. Maul, January 1969.
- \*C&GS 38 Grid Values of Total Magnetic Intensity IGRF—1965. E. B. Fabiano and N. W. Peddie, April 1969.
- C&GS 39 An Advantageous, Alternative Parameterization of Rotations for Analytical Photogrammetry. Allen J. Pope, September 1970. Price \$0.30 (COM-71-00077)
- C&GS 40 A Comparison of Methods for Computing Gravitational Potential Derivatives. L. J. Gulick, September 1970. Price \$0.40. (COM-71-00185)



U.S. DEPARTMENT OF COMMERCE  
Frederick B. Dent, Secretary

NATIONAL OCEANIC AND ATMOSPHERIC ADMINISTRATION  
Robert M. White, Administrator

NATIONAL OCEAN SURVEY  
Allen L. Powell, Director

QC  
801  
U651  
no. 58  
e.2

NOAA Technical Report NOS 58

## Telemetering Hydrographic Tide Gauge

Charles W. Iseley



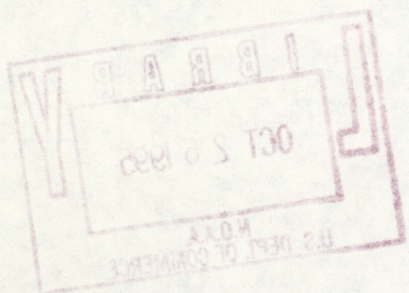
ROCKVILLE, MD.

July 1973

For sale by the Superintendent of Documents, U.S. Government Printing Office, Washington, D.C. 20402. Price 50 cents  
Stock Number 0321-00007

UDC 551.46.081

551.46      Oceanography  
.08      Oceanographic instruments  
.081      Tide gauges



# CONTENTS

	Page
Abstract .....	1
I. Introduction .....	1
A. Purpose .....	1
B. System requirements for Phase I .....	1
C. Summary of progress .....	1
D. Synopsis of results .....	3
II. System components .....	3
A. Telemetering hydrographic tide gauge shore station.....	3
1. Tide signal generation using the NOS bubbler tide gauge .....	4
2. Digital conversion of pressure.....	4
3. Data control and transmission.....	6
B. Shipboard tidal data receiving station .....	7
1. Data recovery.....	7
2. Data output.....	8
III. Equipment system tests and results .....	8
A. Laboratory tests.....	8
B. Preliminary field test .....	11
C. Operational field tests .....	13
IV. Conclusions.....	13
Appendix.....	16
A. Equipment specifications.....	16
1. Transducer .....	16
2. Analog-to-digital converter specifications .....	16
3. Data encoder and decoder specifications .....	16
4. Transceiver specifications.....	16
B. Telemetering link calculations .....	17
C. Decoder error vs. communication channel signal-to-noise ratio.....	17
D. Statistical testing of data samples .....	19

# FIGURES

Figure	Page
1. Functional diagram of the telemetering hydrographic tide gauge system .....	2
2. Shore station instrumentation .....	2
3. Shipboard station instrumentation .....	3
4. NOS bubbler pressure tide gauge.....	4
5. Digital conversion of pressure.....	5
6. Data control and transmission .....	6
7. Shipboard tidal data receiving station .....	7
8. Transducer test equipment configuration .....	8
9. Transducer input-output characteristics.....	9
10. Transducer temperature dependence .....	9
11. Comparative temperature dependence of strain gauge pressure transducers.....	10
12. System test equipment configuration.....	11
13. Total system temperature dependence (shore station).....	11
14. Example of preliminary field test data.....	12
15. Histogram of differences between experimental and standard gauges .....	13
16. Shipboard station installation for operational tests .....	14
17. NOS high speed launch 1257.....	15
18. Signal-to-noise ratio vs throughput rate.....	18
19. Signal-to-noise ratio vs bit error rate .....	18

# Telemetering Hydrographic Tide Gauge

CHARLES W. ISELEY

*Engineering Development Laboratory  
Office of Marine Technology*

**ABSTRACT.**—This report covers phase I of a plan to develop a telemetering hydrographic tide gauge system to provide real-time tidal data to hydrographic survey ships. Phase I included the design, construction, and testing of a telemetering system for use with existing shore-based portable tide gauges. The design requirements for the equipment and the operating characteristics of the system under a field test are described herein.

## I. INTRODUCTION

### A. Purpose

This report describes the first part of the development of a telemetering hydrographic tide gauge system designed to meet the requirements of the National Ocean Survey (NOS) Office of Marine Surveys and Maps to provide real-time tidal data to hydrographic survey vessels. Planned development of the total gauge system was divided into two phases. Phase I of the development, described herein, required the addition of telemetry to existing shore gauges. It involved the design, construction, and testing of a feasibility model. Phase II requires the development of a tide gauge system suitable for open water installation, and so will involve development of a network of ship-deployable buoy gauges with telemetering capability.

### B. System Requirements for Phase I

The features required of the system during phase I development were:

1. On-line (real-time) reporting;
2. self-interrogation through tide level sensing, executing transmissions at operator selectable intervals of 0.1, 0.2, or 0.4 ft of water;
3. a gauge range of 0.0 to 20.0 ft of water;
4. a gauge accuracy of  $\pm 0.1$  ft of water;

5. data output in the form of three-digit BCD data (from shipboard station into automated hydrographic system);
6. a telemetering range of 40 miles; and
7. an operating temperature range of:  
-20° to +55°C for the shore station, and 0° to +55°C for the shipboard station.

### C. Summary of Progress

A feasibility model of a telemetering hydrographic tide gauge meeting the stated requirements was developed by the Engineering Development Laboratory of the National Ocean Survey (NOS). Instrumentation was designed to interface with the NOS field-portable bubbler tide gauge. Figure 1 shows a functional block diagram of the model.

The telemetering hydrographic tide gauge consists of two main components: a transmitting shore station and a receiving shipboard station (figs. 2 and 3). The bubbler pressure tide gauge at the shore station provides a pressure signal that is converted into an electrical signal by a strain gauge pressure transducer. The signal is then digitized, stored, and tested by a threshold-activated keying circuit. The tide level threshold is preselected and corresponds to 0.1, 0.2, or 0.4 ft of water. When the preset threshold is reached, the data are coded into frequency shift keying (FSK) tones and transmitted by

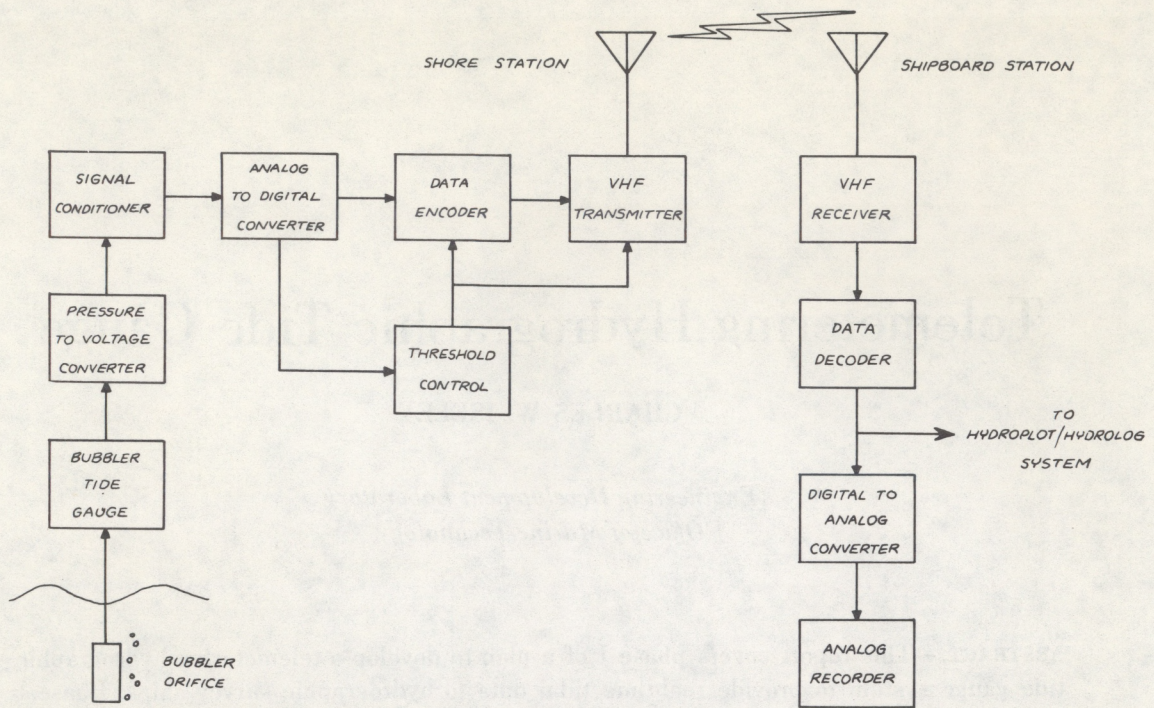


FIGURE 1.—Functional diagram of the telemetering hydrographic tide gauge system.

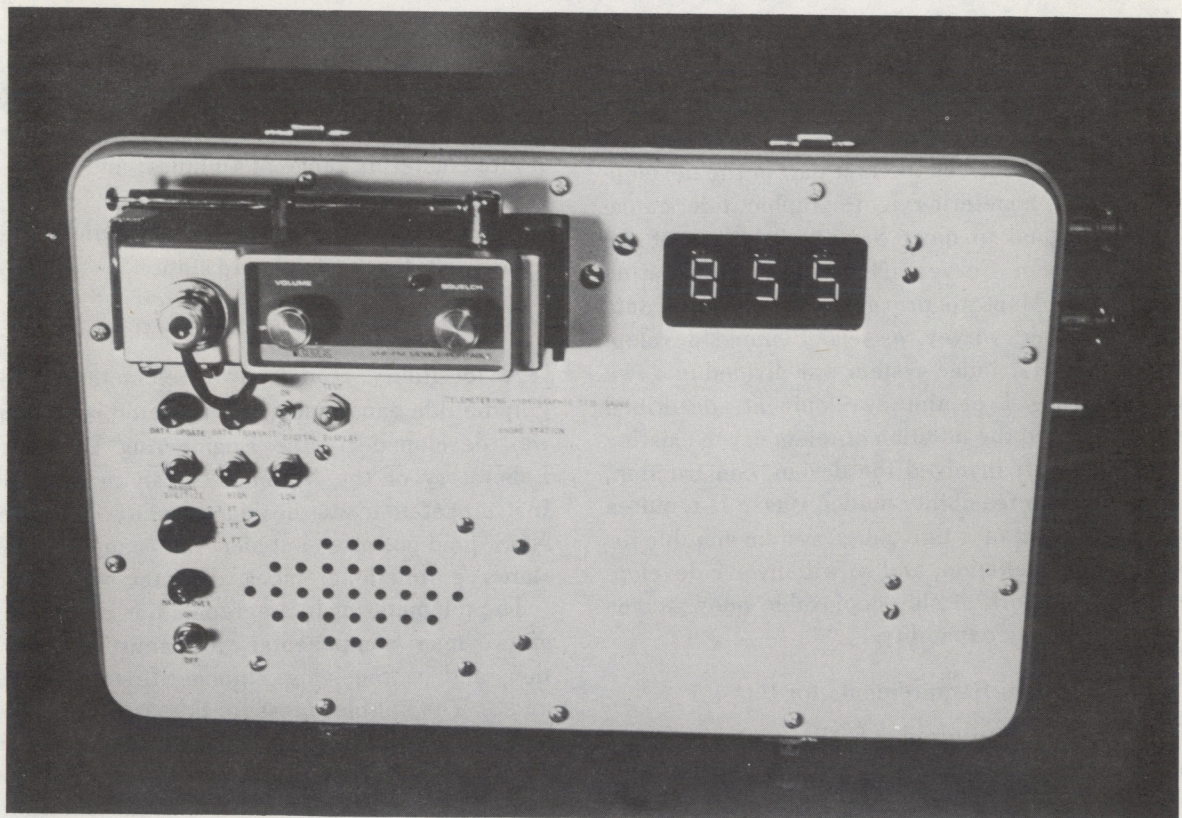


FIGURE 2.—Shore station instrumentation.

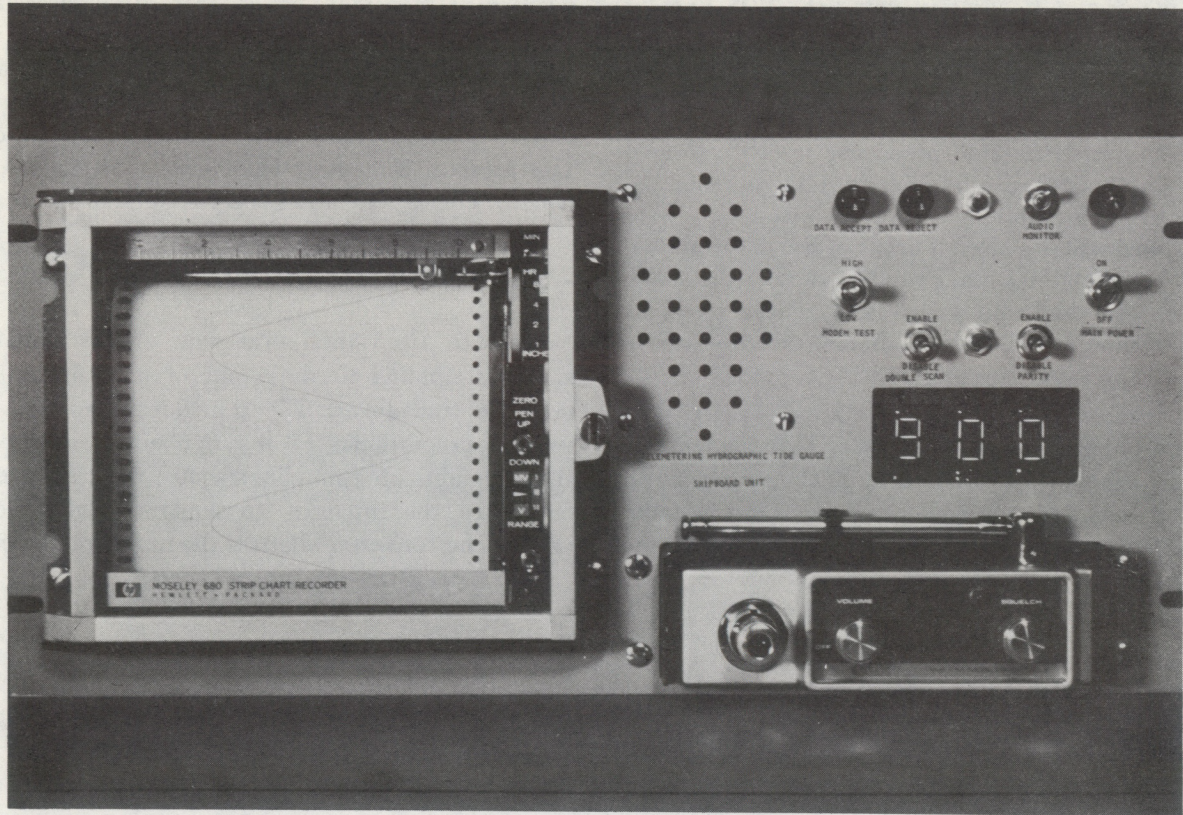


FIGURE 3.—Shipboard station instrumentation.

FM/VHF radio link to the survey vessel. An operating frequency of 40 MHz and transmitter output power of 50 watts were selected to achieve a water path range of 40 miles.

Signals received by the shipboard station are processed to recover the digital data which are then tested for parity and redundancy. If the tests are passed, the transmission process has been validated and the data are released to the shipboard hydroplot/hydrolog system. The shipboard station retains and displays the last sample of telemetered tidal data until the next sample update. In the feasibility model, digital-to-analog conversion of the data also takes place aboard ship and permits logging of data by a strip-chart recorder.

#### D. Synopsis of Results

Laboratory tests showed that pressure transducer error due to temperature contributes less than 0.1 ft to system error over the temperature range specified in the requirements. Transducer hysteresis and non-linearity contribute negligible error.

Further tests, conducted after integration of the

transducer into the shore station equipment, demonstrate that the system maintains calibration to within 0.02 ft of water from  $-30^{\circ}$  to  $+55^{\circ}\text{C}$ .

A 4-week preliminary field test period followed the laboratory testing. During this time the hydrographic tide gauge and a standard tide gauge operated simultaneously. Samples of the differences between the two gauge readings for corresponding times were analyzed statistically. All the sample standard deviations were less than 0.02 ft of water. A constant difference—zero standard deviation—would indicate perfect agreement between the gauges.

## II. SYSTEM COMPONENTS

### A. Telemetering Hydrographic Tide Gauge Shore Station

The shore station consists of instrumentation that digitizes pressure signals from the NOS bubbler tide gauge (fig. 4) and telemeters the data in real time to receiving equipment aboard the hydrographic survey vessel.

## 1. Tide Signal Generation using the NOS Bubbler Tide Gauge.

The NOS bubbler tide gauge was chosen to demonstrate system feasibility because it is:

- a. Currently in widespread use in NOS, so field personnel are familiar with its operation;
- b. easily portable;
- c. adaptable to coastal areas of rough terrain unsuitable for other gauges, such as the standard float-well gauge and gauges requiring pier, piling, or other stable structures above the water surface; and
- d. readily available at NOS marine centers.

The bubbler gauge consists of two elements: a purge system and a mechanical, spring-driven analog recorder. Nitrogen gas pressurized in cylinders provides purge system energy. Bubble rate is

maintained constant by a differential pressure regulator.

The pressure required to keep seawater from entering the orifice and purge line is proportional to the head of water above the bubbler orifice. This pressure is measured by means of a mechanical bellows connected to the recorder pen arm.

## 2. Digital Conversion of Pressure

Pressure from the purge line of the bubbler gauge is applied to the input of a strain gauge pressure transducer. The transducer produces a voltage proportional to the applied pressure. A signal conditioning amplifier scales the transducer output to the input of an analog-to-digital converter. The converter digitizes the input voltage into

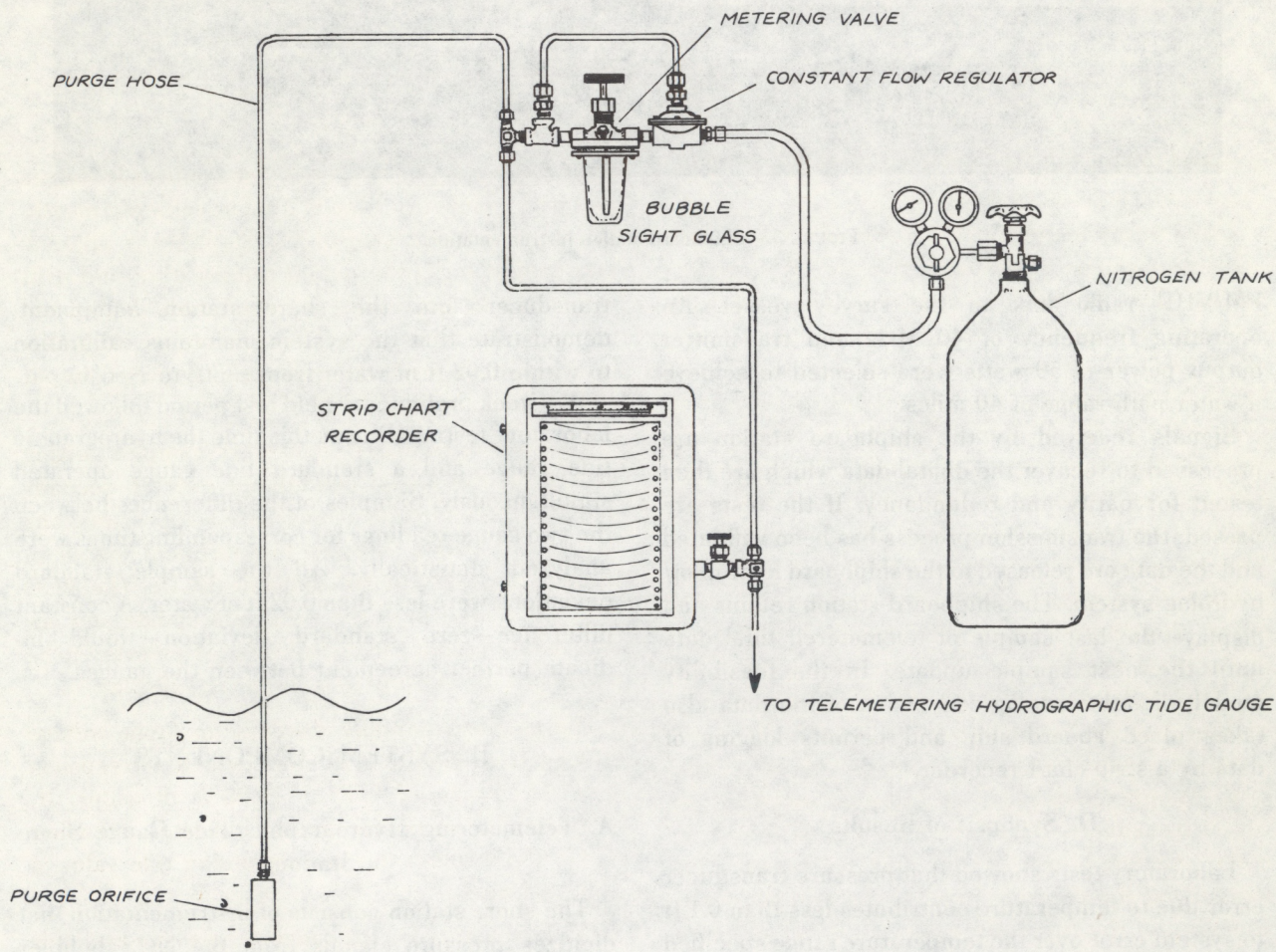


FIGURE 4.—NOS bubbler pressure tide gauge.

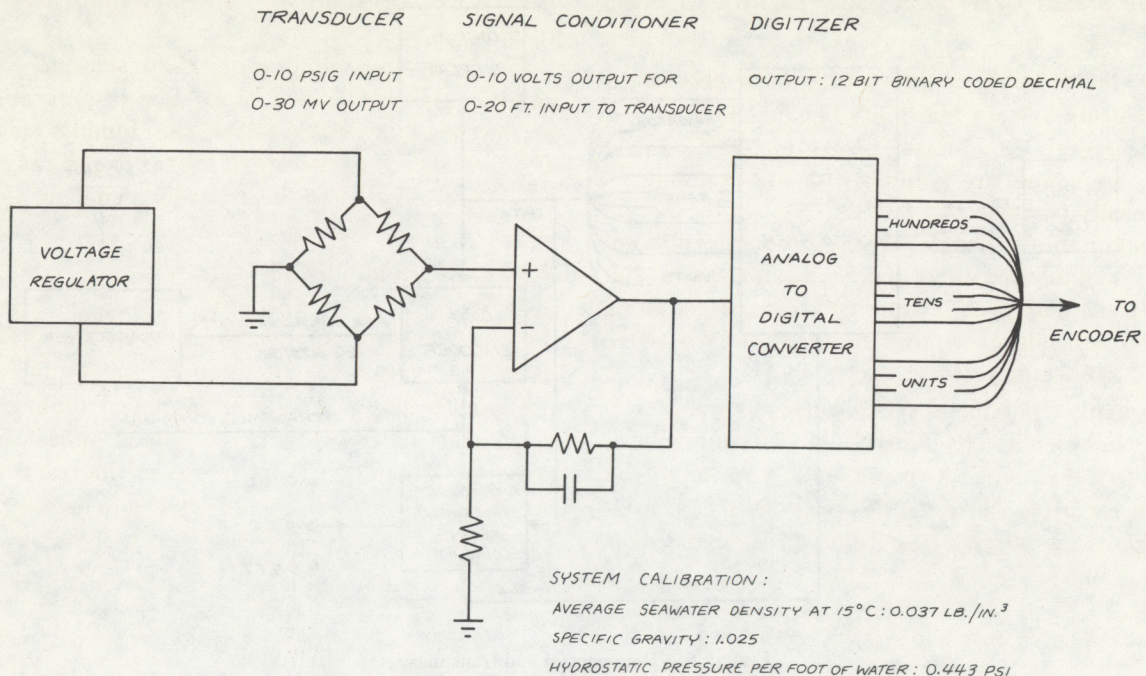


FIGURE 5.—Digital conversion of pressure.

a coded binary output. A functional diagram of the conversion process is shown in figure 5.

The sensing elements of the pressure transducer are strain gauges in a four-active-arm Wheatstone bridge. The bridge excitation voltage is 10 volts d.c. and is regulated. The transducer has a range of 10 psig, which corresponds to a maximum range of 23 ft of seawater. The transducer output for 10 psig input is 30 millivolts. The temperature coefficient of the transducer, as specified by the manufacturer, is 0.0027% of full scale per centigrade degree over an operating range of  $-30^{\circ}$  to  $+50^{\circ}$ C. This translates to an error of 0.0006 ft of water per centigrade degree. Laboratory testing of transducer characteristics was performed. A discussion of the tests and test results is presented in section III. Detailed transducer specifications are given in section A of the appendix.

Signal conditioning is accomplished by a low-drift chopper-stabilized operational amplifier in which transducer output is amplified, or scaled, to make maximum use of the digitizer range. This means that the pressure input to the system, corresponding to the full scale value of 20.0 ft of water, is amplified to coincide with the full scale input requirement of the analog-to-digital converter, or 10 volts d.c.

The amplifier input offset voltage with respect to

temperature is 0.1 microvolt per centigrade degree and with respect to time is 2 microvolts per month. Since the voltage gain of the amplifier is approximately 400 to 1, the actual temperature and drift errors are 40 microvolts per centigrade degree and 0.8 millivolts per month. These errors are negligible in comparison with the full-scale amplifier output of 10.0 volts.

The analog-to-digital converter samples analog data from the signal conditioner every 6 seconds and uses the technique of successive approximations to convert analog voltages to equivalent output in three-digit binary coded decimal (BCD). The BCD data are stored until the next data update and are decoded to permit the digital value of pressure to be presented for viewing as a three-digit display.

The digitizer actually displays an input voltage ranging from 0.00 to 9.99 volts, which corresponds to a tide range of 0.00 to 19.98 ft of water. If, for example, the digital display indicates a reading of 375 (3.75 volts), the corresponding tide value is 7.50 ft of water.

BCD data stored in the converter also are available for logic control functions which select thresholds and perform transmitter keying operations. Detailed specifications of the converter are presented in section A of the appendix.

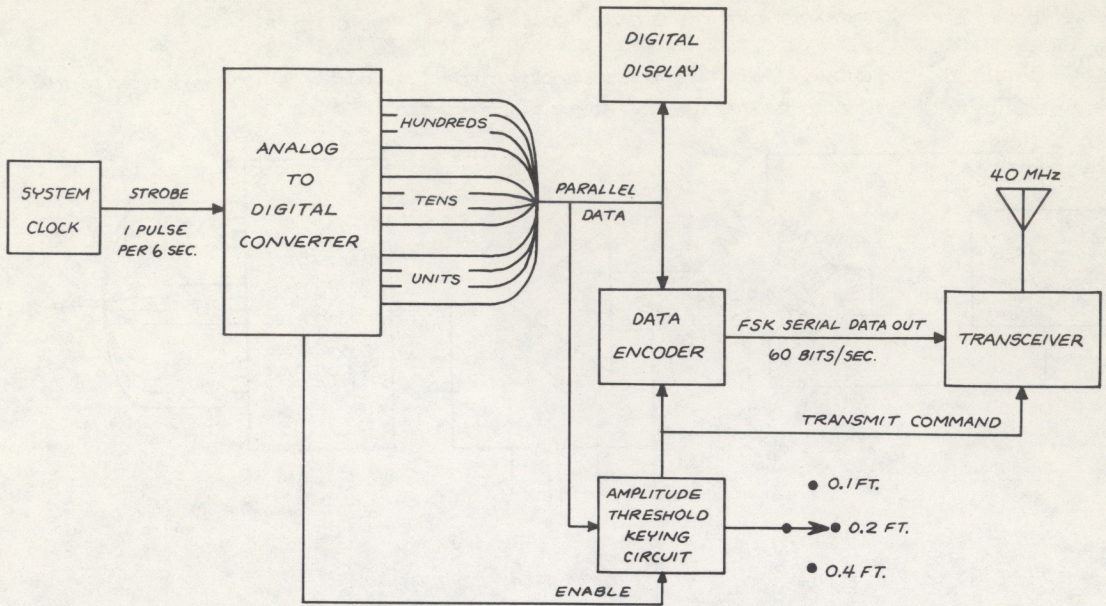


FIGURE 6.—Data control and transmission.

### 3. Data Control and Transmission

Tide data in digital form are monitored by the threshold keying circuit for selected amplitude interval transmission. Data for transmission are formed into a serial word by the data encoder which uses frequency shift keying to modulate the transmitter. A functional block diagram of the data control and transmission components is shown in figure 6.

At present, tide gauge data are logged either continuously (as in the case of analog recording gauges), or at timed intervals (as with digital gauges). However, for the purpose of correcting hydrographic soundings in real time, the tide data are not actually required until the tide has changed by an amount that causes the soundings to be in error. The technique of telemetering data to the vessel only when a significant change has taken place simplifies the shore station operation by eliminating the need for a real-time clock and also conserves shore station power by ensuring minimal use of the transmitter.

When the shore station is set up, an operator selects the desired amplitude interval on the instrument control panel (0.1, 0.2, or 0.4 ft of water). This quantity corresponds to the tidal amplitude change that must take place before a data transmission occurs. The value selected is dependent

upon the tidal range of the area and the amount of tidal change that can be tolerated before a sounding correction is required.

Data control is accomplished by the amplitude threshold keying circuit. The keying circuit consists of gating and storage elements that monitor the output of the analog-to-digital converter. Transmission of data occurs only when certain numerical relationships corresponding to the interval selection are satisfied. Once a data word has been transmitted, the circuit inhibits repeated transmissions until the tide has changed by a preset value (0.02 ft of water).

Before the data are transmitted, they are encoded into a 76-bit word that includes two repetitive tide data scans, parity coding for error detection, and timing pulses for data recovery synchronization. The encoder input is parallel and the output is serial.

The data output takes the form of a serial train of binary transitions between two tones (frequency shift keying—FSK) and is used to modulate the transmitter. The FSK transition frequencies (1440 and 1800 Hz) are generated at a rate of 60 bits per second. The time required for transmission of a complete data word is approximately 1 second. Detailed encoder specifications are given in section A of the appendix.

The shore station transmitter and shipboard receiver are identical transceivers. Microphones pro-

vided with the system permit two-way voice communication between the shore and shipboard stations to facilitate checking of the data link and overall system operation during station setup. Voice communications, other signals, and noise do not create erroneous data reception at the shipboard station because the data recovery instrumentation responds only to FSK modulation in a predetermined format.

Because the transmitter and receiver are identical units, two modes of operation are possible. In the present operating mode, the shore station transmits only, and the shipboard station receives only. Addition of interrogation circuitry would give the ship the capability of calling any one of many shore stations for data reports.

The transmitter for the system operates on the assigned frequencies of 40.27 or 40.29 MHz and uses narrow-band frequency modulation (FM). Output power into the antenna is 50 watts (rms). Detailed specifications of the transceiver are presented in section A of the appendix.

Quarter wave omnidirectional ground plane antennas are used with both shore and ship installation. The antennas are rugged and designed especially for marine applications.

Propagation calculations have shown that a 40-mile water path telemetering range for the system

is feasible. Details of the link calculations are given in section B of the appendix.

## B. Shipboard Tidal Data Receiving Station

Shipboard receiving station operation is essentially passive. FM signals received by the shipboard transceiver are immediately introduced into the data decoder for tidal data recovery. Decoded data are made available to the automated hydrographic system at this stage and also are displayed for viewing. A block diagram of the shipboard receiving station is shown in figure 7.

### 1. Data Recovery

The function of the shipboard station receiver is to monitor the telemetry channel continuously. When data are being received, they can be heard over the shipboard station speaker or they can be muted. (The tidal data FSK tone burst sounds like the ringing of a telephone.) A received serial FSK data word is converted by the data decoder to the original binary form. The word is then stored in a register until parity and double scan tests are completed. If the tests are passed, the data word is released to the output storage register and is made available to the hydroplot/hydrolog system. Decoder specifications are given in detail in section A of the appendix. A discussion of decoder error occurrence as a function

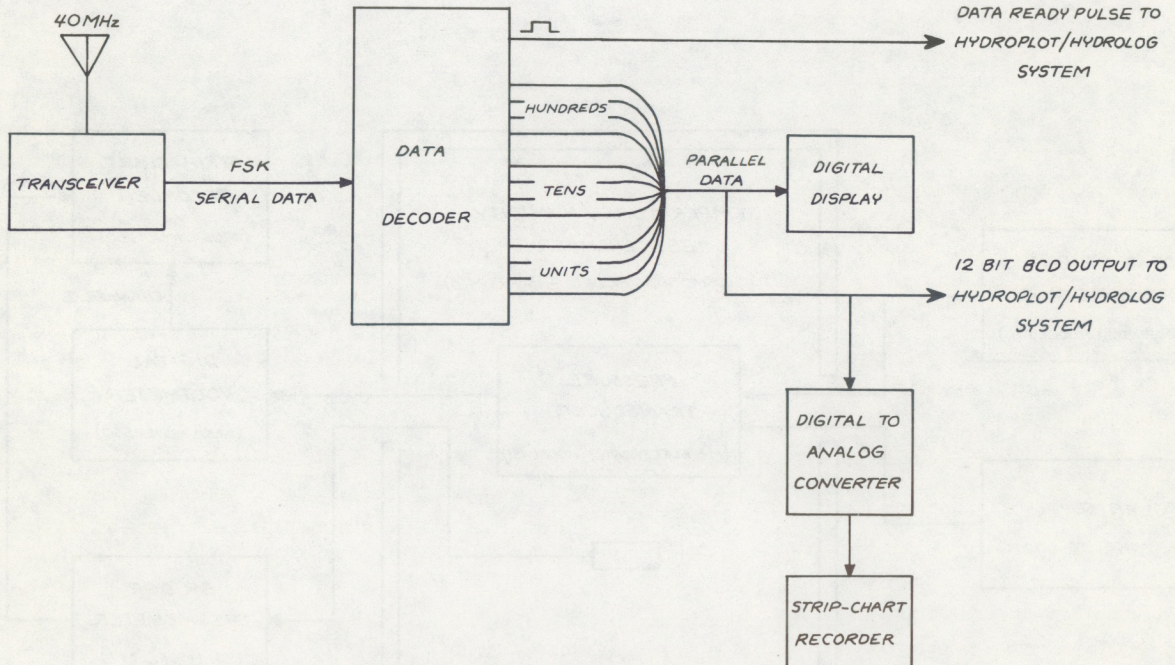


FIGURE 7.—Shipboard tidal data receiving station.

of transmission link signal-to-noise ratio is given in section C of the appendix.

## 2 Data Output

A "data ready" output pulse signals the hydroplot/hydrolog system when the tidal data have been updated. The data are stored until the next transmission is received. The BCD data output is normally in positive logic. However, the output can be switched to inverted positive logic as required for certain NOS automated hydrographic systems. Stored tidal data in the decoder also are displayed for viewing as three decimal digits on the front panel of the shipboard station. Digital-to-analog conversion of the data is available for presentation on a strip-chart recorder at the operator's discretion. Although not specified in the requirements, the digital-to-analog converter and strip-chart recorder were added to the feasibility model to permit quick checking of accumulated tidal data independent of the hydroplot/hydrolog system.

Simple self-test provisions for the shipboard station have been included. These tests permit an operator to check out all equipment on the decoder output by forcing all output bits to binary 0 or 1. A self-test of the visual readout display has also been incorporated.

## III. EQUIPMENT SYSTEM TESTS AND RESULTS

### A. Laboratory Tests

Preliminary tests were conducted on the shore station pressure transducer before final integration into the system to determine temperature dependence, linearity, and hysteresis. Two transducers for the feasibility model were tested in the manner illustrated in figure 8.

The transducer was placed in the temperature test chamber and subjected to temperature and pressure cycling. Input pressure was controlled by a pneumatic dead-weight pressure gauge. The pressure was varied in 1-psi increments over a range from 0 to 12 psi. Transducer excitation was provided by a constant voltage power supply; transducer output was monitored by a digital voltmeter. Analog output from the digital voltmeter was recorded on channel I of a 2-channel strip-chart recorder. The temperature test chamber was operated over the range from  $-30^{\circ}$  to  $+55^{\circ}\text{C}$  at stabilized temperature intervals approximately  $10^{\circ}\text{C}$  apart. Chamber temperatures were measured by a thermistor bridge thermometer and recorded on channel II of the strip-chart recorder.

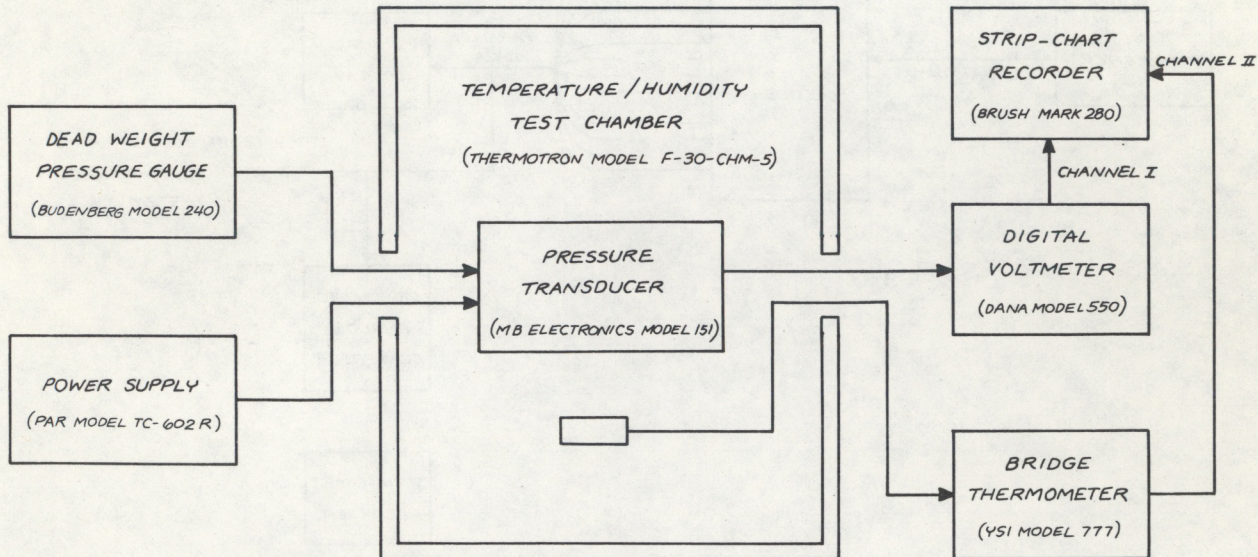


FIGURE 8.—Transducer test equipment configuration.

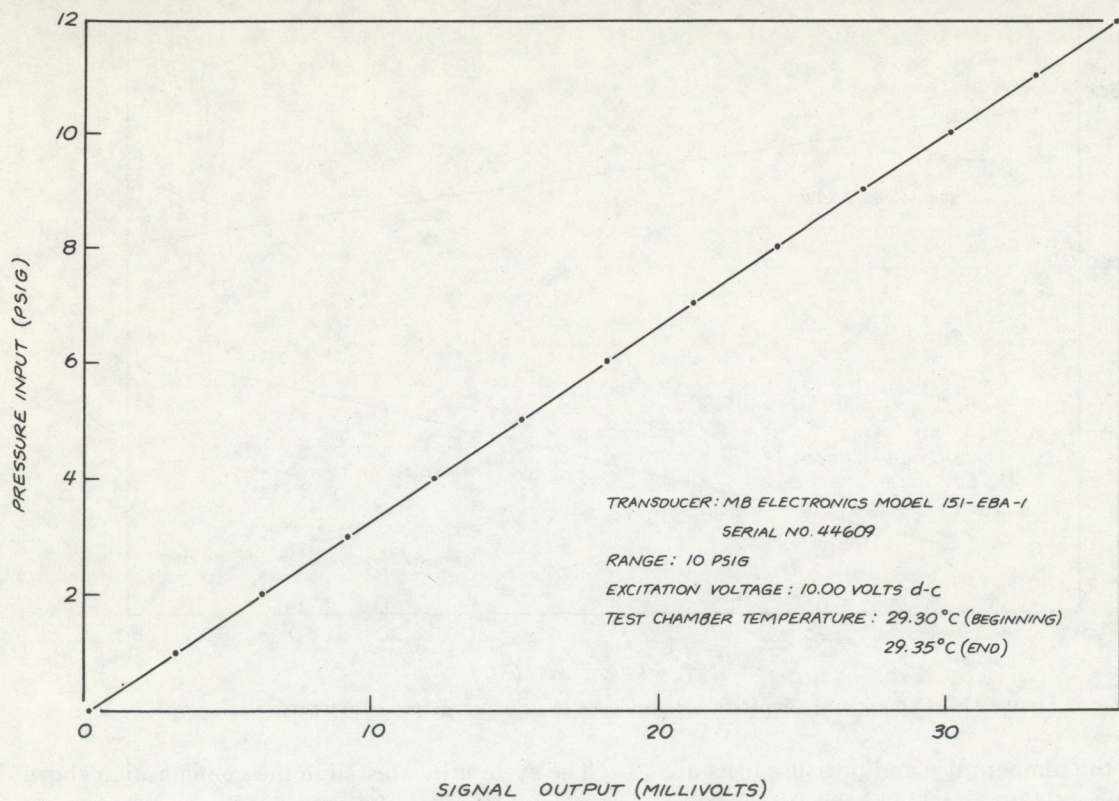


FIGURE 9.—Transducer input-output characteristics.

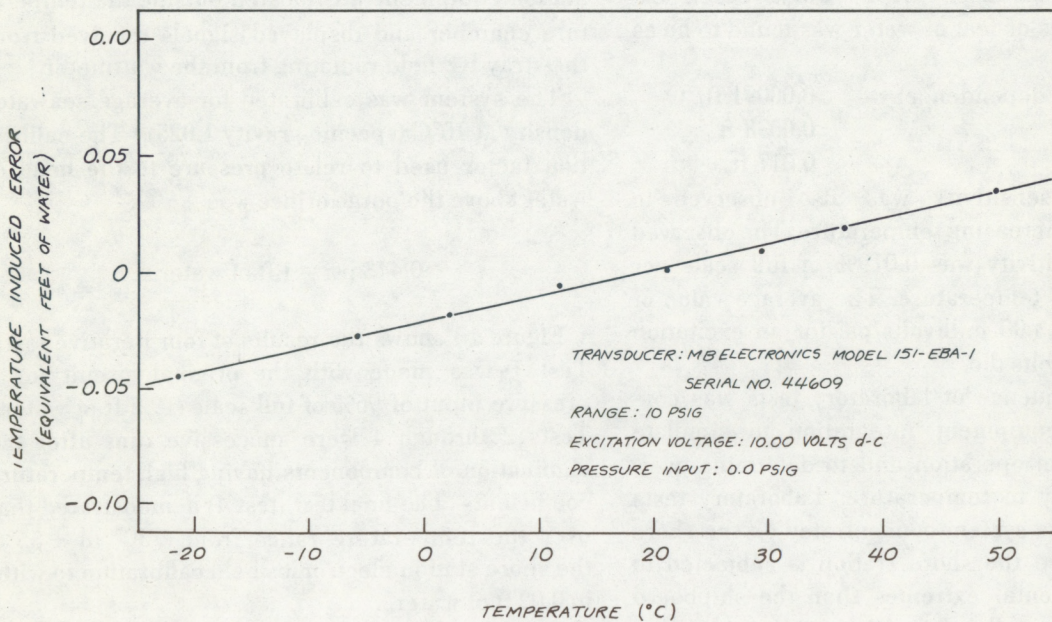


FIGURE 10.—Transducer temperature dependence.

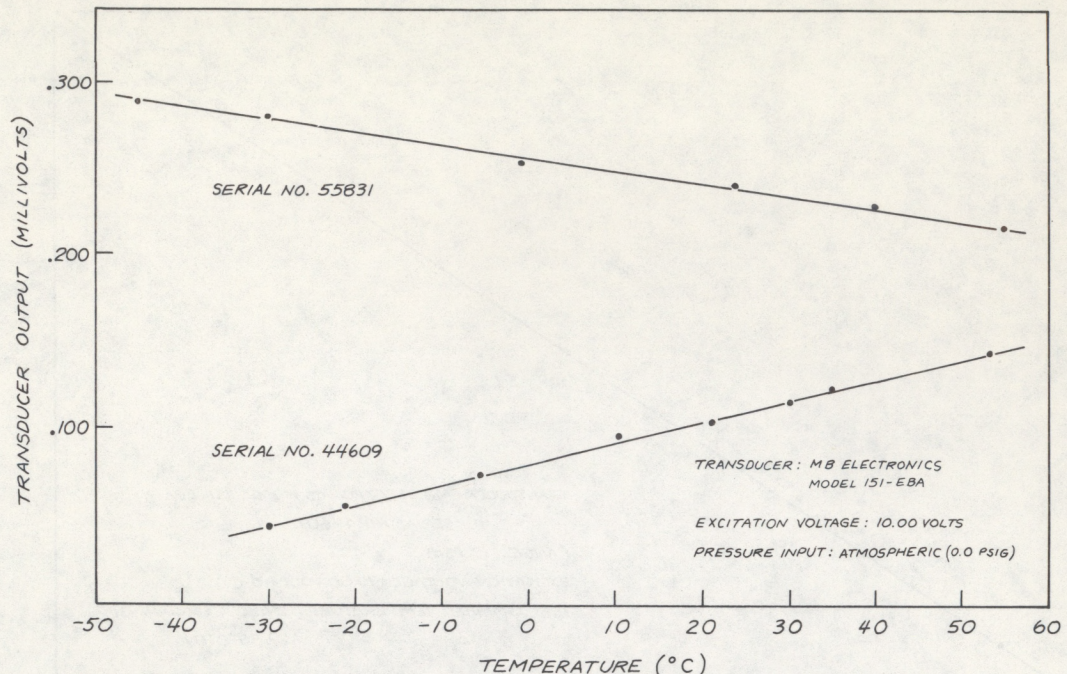


FIGURE 11.—Comparative temperature dependence of strain gauge pressure transducers.

Results of the temperature and pressure tests are shown in figures 9, 10, and 11. Figure 9 presents a plot of transducer input/output characteristics. Figure 10 shows the temperature-induced error of a transducer in terms of feet of water. Figure 11 shows a comparative plot of the temperature dependency of the two transducers tested.

Measured transducer error (worst case), expressed in terms of feet of water was found to be as follows:

temperature dependence:	0.00091 ft/°C
hysteresis:	0.0038 ft
non-linearity:	0.017 ft

Transducer sensitivity was also observed to decrease with increasing temperature. The observed change in sensitivity was 0.019% of full scale per 10°C change in temperature. The average value of sensitivity was 3.00 millivolts/psi for an excitation voltage of 10.0 volts d.c.

The next sequence of laboratory tests was conducted after equipment integration to simulate complete system operation and to determine overall susceptibility to temperature. Laboratory tests of the tide gauge system concentrated on the shore electronics since the shore station is subjected to more environmental extremes than the shipboard unit, which is usually placed in an air-conditioned environment adjacent to the hydroplot/hydrolog system.

The system was tested in the configuration shown in figure 12. The shore station was placed in the temperature test chamber and cycled from  $-30^{\circ}$  to  $+55^{\circ}\text{C}$ . Calibration reference pressure was maintained by the dead weight pressure gauge. The shore station transmitter output terminal was connected to an absorption wattmeter. The shipboard station equipment was located outside the temperature chamber and displayed signals received from the stray RF field radiating from the wattmeter.

The system was calibrated for average seawater density at  $15^{\circ}\text{C}$  (specific gravity 1.025).<sup>1</sup> The calibration factor used to relate pressure to the head of water above the purge orifice was

$$0.443 \text{ psi} = 1 \text{ ft of water.}$$

Figure 13 shows the results of four iterative tests. Test 1 was made with the original circuit for a pressure input of 96% of full scale (19.2 ft of water.) Tests 2 through 4 were successive runs after the elimination of components having high temperature coefficients. The final test (test 4) demonstrated that over the temperature range from  $-30^{\circ}$  to  $+55^{\circ}\text{C}$  the shore station electronics held calibration to within 0.02 ft of water.

<sup>1</sup> Derived from "Atlantic Coast Density Tables," C&GS Publication 31-2.

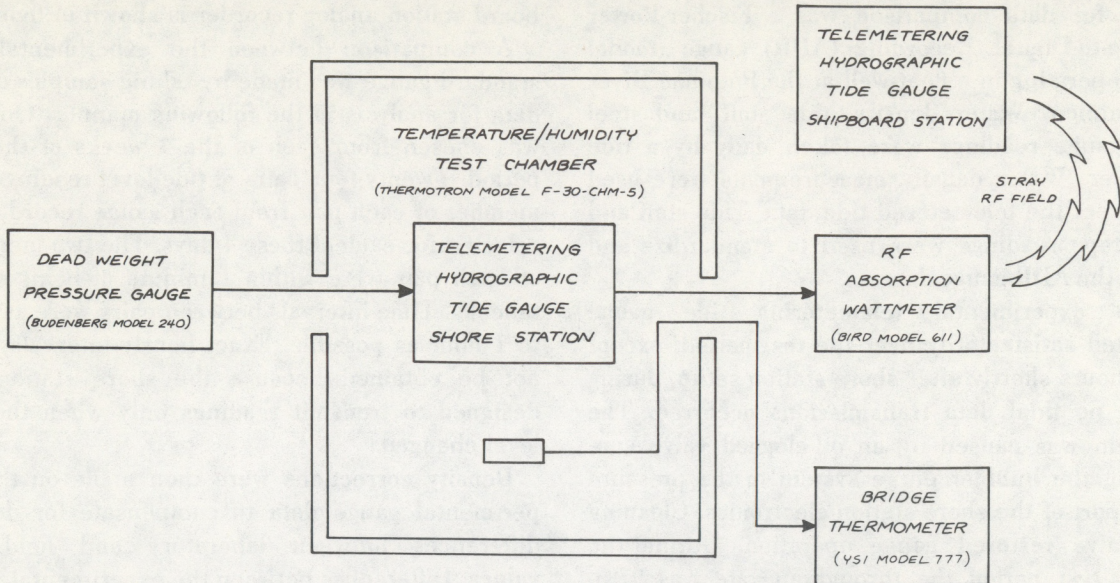


FIGURE 12.—System test equipment configuration.

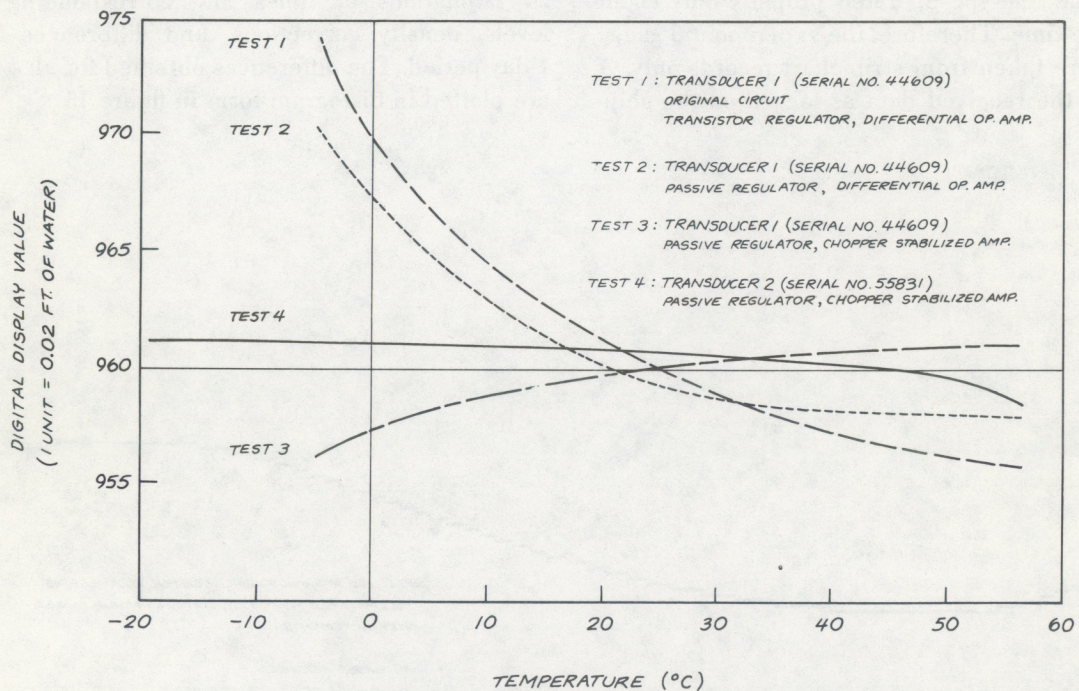


FIGURE 13.—Total system temperature dependence (shore station).

## B. Preliminary Field Test

A preliminary field test of the telemetering hydrographic tide gauge was conducted in December 1971 to work out possible operating problems before the system was introduced for operational tests on a hydrographic survey vessel. For the test, the shore station was installed at the Washington,

D.C. tide station on the Potomac River and data were telemetered to the Washington Science Center in Rockville, Maryland, for a period of 4 weeks. The shipboard receiving station was connected to a simulated hydrographic data logging system. Digital time and received tide data were logged by teletype printout. There also was continuous analog recording of the received data. The reference, or standard

gauge for data comparison was a Fischer-Porter Analog-to-Digital Recording (ADR) gauge (model 1550) operating in a float-well at the Potomac River tide station. Water density, tide staff, and steel tape gauge readings were taken daily by a tide observer. Water density measurements were used to correct the telemetered tide data. Tide staff and steel tape readings were used to standardize and check the ADR gauge data.

The experimental telemetering tide gauge operated satisfactorily over the test period, except for 4 hours shortly after shore station setup, during which no tidal data transmissions occurred. The problem was caused by an oil-clogged valve connecting the bubbler purge system to the pressure input port of the shore station electronics. Cleaning the valve restored gauge operation. During the 30-day test period the throughput rate was 97%, i.e., 97% of all data words transmitted were received. The teletype hard copy was not continuous because the teletype operated properly only about 25% of the time. Therefore, the experimental gauge results were taken from strip-chart records only. A sample of the received data as logged on the ship-

board station analog recorder is shown in figure 14.

A comparison between the experimental and standard gauge was made by taking samples of test data for analysis in the following manner: One day was chosen from each of the 4 weeks of the test period. Twenty-four pairs of tide-level readings, one member of each pair from each gauge record, were selected for each of these 4 days. The two members of each pair were within 1 minute of being simultaneous. Time intervals between pairs were as close to 1 hour as possible. Exact hourly intervals could not be obtained because the shore station was designed to transmit readings only when the tide level changed.

Density corrections were then made on the experimental gauge data to compensate for density differences between laboratory and field test values. Differences between the experimental gauge and the standard gauge readings were tabulated. Columns 1 through 5 of table 1 in the appendix show 24 tabulations of times and corresponding tide levels, density corrections, and differences for a 1-day period. The differences obtained for all 4 days are plotted in histogram form in figure 15.

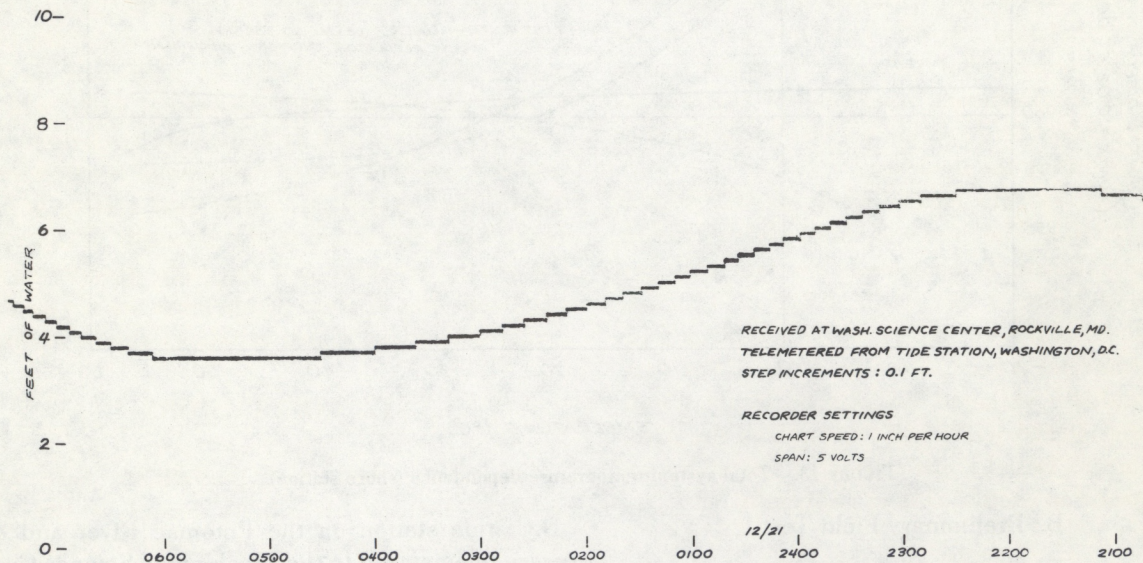


FIGURE 14.—Example of preliminary field test data.

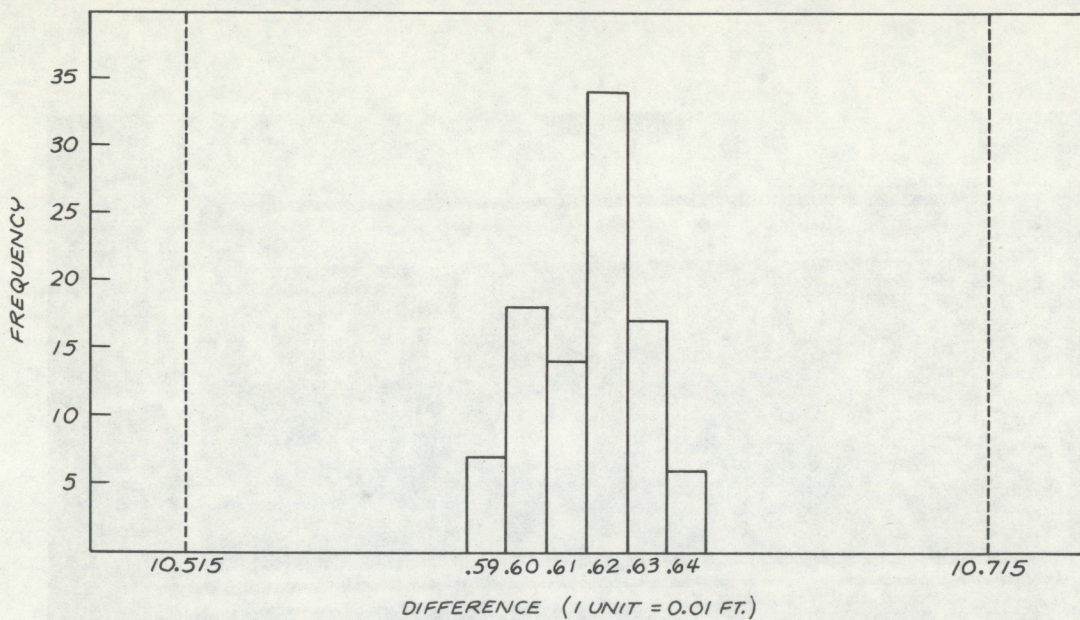


FIGURE 15.—Histogram of differences between experimental and standard gauges.

The four samples of 24 differences each were subjected to a simple statistical test. The t-test was chosen because it tests a hypothesis on the population mean using the sample mean and sample standard deviation. The mean of the four sample means was chosen as an estimate of the population mean. "Population" in this case refers to the set of *all* differences that existed during the entire period of simultaneous operation of the experimental and standard gauges, not just the differences tabulated during the field test.

The four sample means were: 10.610, 10.618, 10.616, 10.618. The mean of these values, 10.616, was the estimate to be tested. The four standard deviations were: 0.016, 0.015, 0.012, 0.011. Note that all standard deviations were less than 0.02, which indicates a fairly close grouping of the data. The t-statistic obtained for all four samples indicated that 10.616 was a valid estimate of the population mean. Detailed discussion of the statistical test appears in section D of the appendix.

### C. Operational Field Tests

Preparation for operational testing of the telemetering hydrographic tide gauge began in January, 1972. For the test, the shipboard station was installed into the hydroplot system console on the NOS High Speed Launch No. 1257. The station

antenna was installed on the stern. Figure 16 shows the equipment rack containing the shipboard station and a portion of the hydroplot system. Figure 17 shows a photograph of the High Speed Launch while underway.

At the time this report was written, the final field tests were still in progress. The results of the tests will be published later in an addendum to this report. Data from the operational tests will be analyzed and the results will be used to help formulate the basis of future operational requirements. Operational evaluation of the total system will include a determination of the necessity of including the analog recorder and the audio monitor in the shipboard unit. If these components are not needed, a cost saving and higher reliability can be realized.

### IV. CONCLUSIONS

Laboratory tests and preliminary field tests indicate that the feasibility model of the telemetering hydrographic tide gauge meets the requirements defined for phase I. Tests demonstrating the range of the telemetering system have not been conducted, but will be included in the final field testing. Present plans are to procure production units of the system following evaluation of the final field tests.

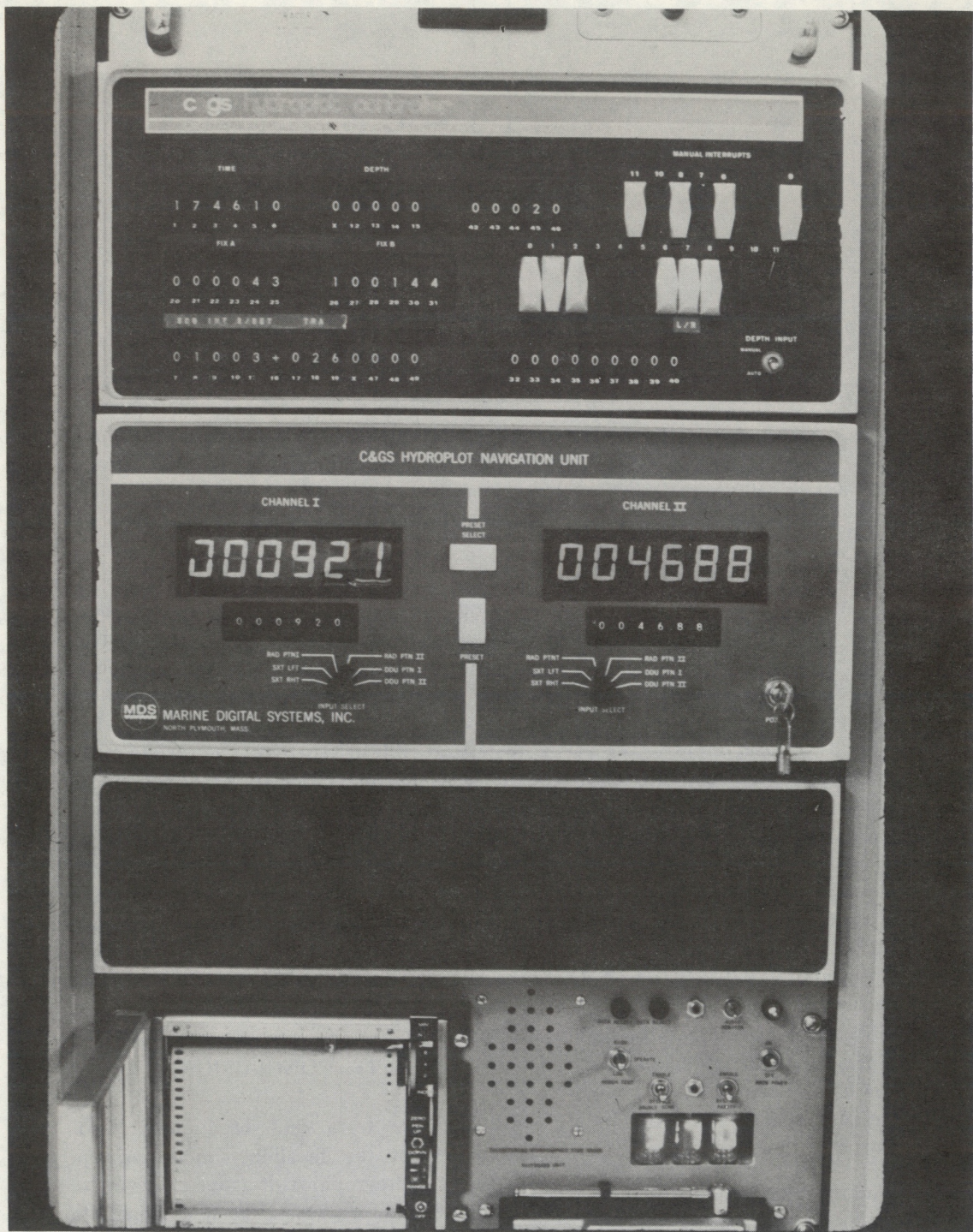


FIGURE 16.—Shipboard station installation for operational tests.



FIGURE 17.—NOS high speed launch 1257.

## APPENDIX

### A. Equipment Specifications

#### 1. Transducer

Manufacturer: M. B. Electronics of New Haven, Connecticut

Model number: 151-EBA-260

Range: 0 to 10 psig

Full scale sensitivity:  $3.0 \text{ mV/V} \pm 0.25\%$

Nonlinearity:  $\pm .10\%$  of full scale (maximum)

Hysteresis:  $0.1\%$  of full scale (maximum)

Nonrepeatability:  $\pm 0.05\%$  of full scale (maximum)

Combined error (nonlinearity, hysteresis and non-repeatability):  $\pm 0.15\%$  of full scale (maximum)

Compensated temperature range:  $-30^\circ \text{ to } +50^\circ\text{C}$

Sensitivity shift with temperature:  $\pm 0.0027\%$  per centigrade degree

Zero pressure output shift with temperature:  $\pm 0.0027\%$  of full scale per centigrade degree.

Input resistance:  $350 \text{ ohms} \pm 3.5 \text{ ohms}$

Output resistance:  $350 \text{ ohms} \pm 3.5 \text{ ohms}$

Input voltage: 10 volts a.c. or d.c.

Insulation resistance: 5,000 megohms at 50 volts

Safe overpressure: 2,000% of full scale

#### 2. Analog-to-Digital Converter Specifications

Manufacturer: Analog Devices, Inc., of Cambridge, Massachusetts

Model number: ADC12QM/BCD/ET

Resolution: 3-digit binary coded decimal

Accuracy:

Relative:  $\pm 1/2$  least significant bit

Quantization:  $\pm 1/2$  least significant bit

Temperature coefficient:

Gain:  $\pm 5 \text{ ppm/C}^\circ$  of reading

Zero:  $\pm 5 \text{ ppm/C}^\circ$  of full scale

Conversion time: 25 microseconds maximum

Input voltage range: 0 to +10 volts d.c.

Input impedance: 100 megohm

Output signals: parallel binary coded decimal, TTL, DTL compatible

Power requirements: 25 milliamperes at +15 volts d.c., 35 milliamperes at -15 volts d.c., 200 milliamperes at 5 volts d.c.

Operating temperature range:  $-55^\circ \text{ to } +125^\circ\text{C}$

#### 3. Data Encoder and Decoder Specifications

Manufacturer: Larse Corporation of Palo Alto, California

Data encoder model: LCS-150-FSK

Data decoder model: LCR-250-FSK

Center frequency: 1620 Hz ( $\pm 180 \text{ Hz}$ )

Data rate: 60 bits per second

Encoder output impedance: 600 ohms

Decoder input impedance: 600 ohms

Data input and control function logic compatibility: DTL and TTL

(logic 1: +2.5 to +5 volts)

(logic 0: 0 to +0.5 volts)

Data input/output: 14 parallel data inputs into encoder (parity coding is included); 14 parallel data outputs from decoder

Transmission mode: double scan transmission with parity (76 bits/transmission)

Total time required before data are released at output of decoder: 1.2 seconds

Power requirements:

Data encoder: 40 milliamperes maximum at 12 volts d.c., 70 milliamperes maximum at 5 volts d.c.

Data decoder: 40 milliamperes maximum at 12 volts d.c., 20 milliamperes maximum at 5 volts d.c.

Operating temperature range:  $-30^\circ \text{ to } +75^\circ\text{C}$

#### 4. Transceiver Specifications

Manufacturer: Repco, Inc., of Orlando, Florida

Model number: MPN3L22Q

General:

Operating frequency: 40.27 and 40.29 MHz

Number of channels: 2

Power requirements:

Transmit: 9.0 amperes at 13.8 volts d.c.

Receive: 0.785 amperes at 13.8 volts d.c.

Standby: 0.150 amperes at 13.8 volts d.c.

Operating temperature range:  $-30^\circ \text{ to } +60^\circ\text{C}$

Transmitter:

R-F output power: 50 watts (rms)

Spurious and harmonic emission: 63 dB below carrier

Frequency stability:  $\pm 0.002\%$  from  $-30^\circ \text{ to } +60^\circ\text{C}$

Modulation: narrow band ( $\pm 5 \text{ kHz}$ )

FM noise: -50 dB at 2/3 system deviation

Emission: 16F3

Receiver:

Selectivity:  $-80 \text{ dB} \pm 25 \text{ kHz}$  (EIA two signal method)

Sensitivity: 0.35 microvolts for 20 dB signal-to-noise ratio at receiver output, 0.25 microvolts for 12 dB signal-to-noise ratio at receiver output

## B. Telemetering Link Calculations

System requirements specify a telemetering range of 40 miles. The following computations were made to determine the feasibility of a 40-mile water path telemetering range.

The transmitting and receiving antennas are identical and assumed to be ideal nondirective (isotropic) radiators. For the calculations, an antenna height of 30 feet is used for both the transmitting and receiving antennas. Antenna impedance is 50 ohms. The radiating power of the transmitting antenna is taken to be 50 watts. Minimum allowable receiver output signal-to-noise (S/N) ratio is taken to be 12 dB, which corresponds to an input signal of 0.25 microvolts.

The minimum receiving antenna power to produce a receiver output S/N ratio of 12 dB is:

$$P_r = \frac{(V_r)^2}{Z_r}$$

$$P_r = \frac{(2.5 \times 10^{-7})^2}{50}$$

$$= 1.25 \times 10^{-15} \text{ watts}$$

where  $P_r$  = receiver power

$V_r$  = receiver voltage

$Z_r$  = receiving antenna impedance

The maximum allowable propagation path loss for  $P_r = 1.25 \times 10^{-15}$  watts is

$$\frac{P_r}{P_t} = \frac{1.25 \times 10^{-15}}{50}$$

$$= 2.5 \times 10^{-17} \text{ or } -166 \text{ dB}$$

where  $P_t$  = radiated power

The path loss over plane earth for a distance of 40 miles is given by:<sup>2</sup>

$$\frac{P_r}{P_t} = \left( \frac{h_1 h_2}{d^2} \right)^2 g_t g_r$$

where  $h_1, h_2$  = transmitting and receiving antenna height (ft.)

$d$  = distance (ft.)

$g_t, g_r$  = transmitting and receiving antenna power gain.

( $g_t = g_r = 1$  for isotropic antennas)

However, the minimum effective antenna height ( $h_0$ ) for the shipboard station antenna operating at 40 MHz over seawater is 160 ft.<sup>2</sup> Thus the calculated propagation path loss for plane earth is:

$$\frac{P_r}{P_t} = \left\{ \frac{(30)(160)}{[(40)(5280)]^2} \right\}^2 \cong 1 \times 10^{-14} = -140 \text{ dB}$$

Diffraction loss resulting from earth curvature over seawater (relative to plane earth) at 40 MHz and a distance of 40 miles for vertically polarized antennas is -6 dB. (Assumptions: earth is a perfect sphere and ratio of effective earth radius to true is 4/3.)<sup>3</sup> The calculated propagation loss with correction for curved earth at 40-mile range is -146 dB.

Conclusion: The calculated propagation path loss is 20 dB less than the maximum allowable propagation path loss for the system. Therefore, operation at 40 miles is feasible.

## C. Decoder Error vs. Communication Channel Signal-To-Noise Ratio

Data errors that arise from the telemetering process between the shore station and shipboard station can be categorized into two forms: *throughput rate* and *bit error rate*. Throughput rate gives an indication of the amount of data words lost in the transmission process; it is defined as the ratio (expressed as a percentage) between the number of data words received and accepted as valid by the decoder and the total number of words transmitted. If, for example, the RF signal fades during a transmission so that only part of a data word is received, the entire word is rejected by the decoder; for that particular transmission, the throughput rate is zero. If, on the average, one out of ten transmitted words is either rejected or not received, the throughput rate is 90%.

<sup>2</sup> Kenneth Bullington, "Radio Propagation Fundamentals", Antenna Engineering handbook pp. 33-4, McGraw Hill, 1961.

<sup>3</sup> Ibid, nomogram, page 33-6.

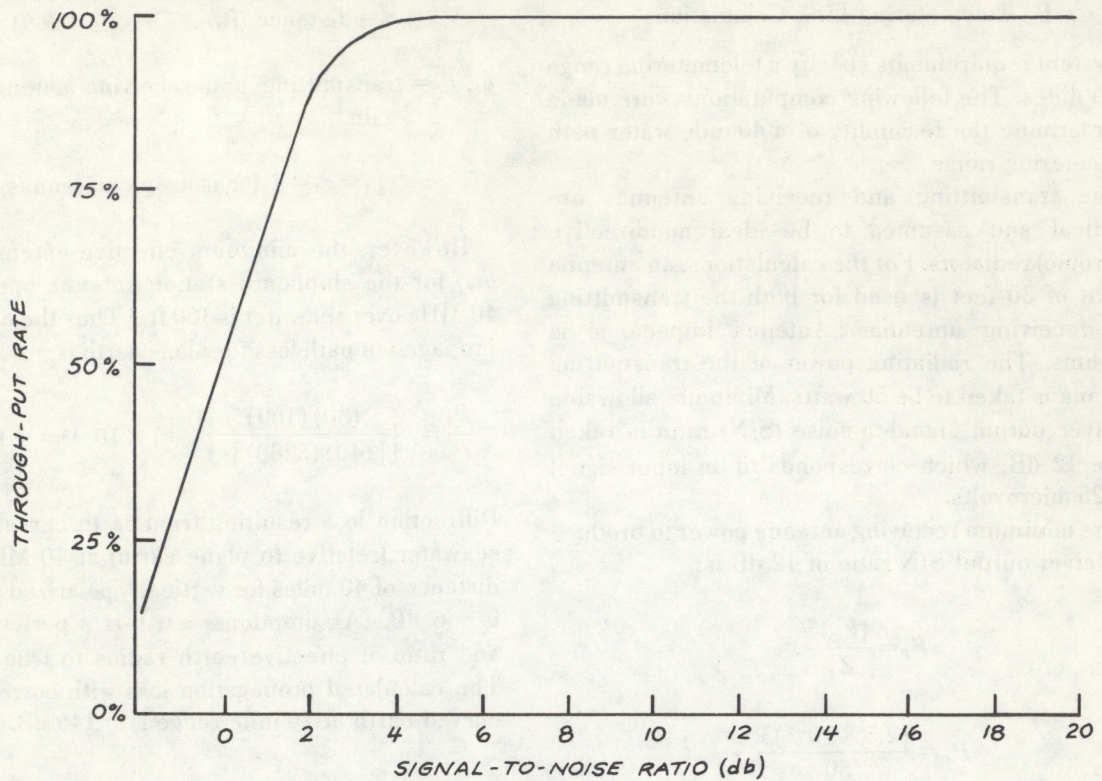


FIGURE 18.—Signal-to-noise ratio vs throughput rate.

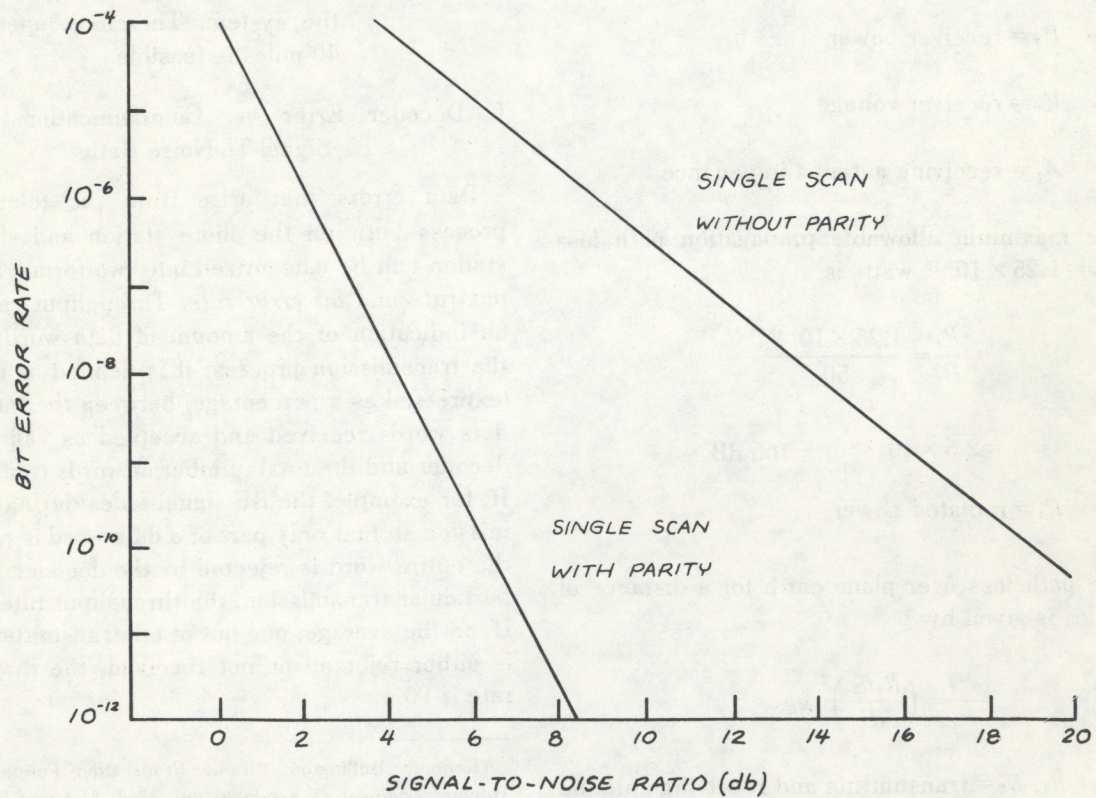


FIGURE 19.—Signal-to-noise ratio vs bit error rate.

A data word from the decoder may be valid or may contain undetected bit-reversal errors. The frequency of undetected errors in the received data word is the bit-error rate. The bit-error rate is defined as the number of erroneous bits accepted by the decoder compared to the total number of bits accepted. Both throughput and bit-error rates are quantitative indicators of the reliability of the telemetering process as a function of the signal-to-noise ratio of the communication channel. Data supplied by the manufacturer of the data encoder and decoder were plotted to illustrate the relationship of throughput and bit-error rate to channel signal-to-noise ratio (figs. 18 and 19).

The significance of figures 18 and 19 may be demonstrated by considering the signal-to-noise ratio produced by the lowest usable input signal to the receiver (receiver sensitivity threshold). An input signal of 0.25 microvolts yields a 12-dB signal-to-noise ratio at the receiver output. According to figure 18, the throughput rate for a signal-to-noise ratio of 12 dB is, for all practical purposes, 100%. The corresponding bit-error rate for the least secure decoder operating mode (i.e., single scan without parity) is one bit error out of  $1.5 \times 10^7$  bits (fig. 19). For the next more secure operating mode (single scan with parity), the projected rate of undetected bit errors is less than  $10^{-14}$  for a signal-to-noise ratio of 12 db. The two remaining decoder operating modes (i.e., double scan without parity and double scan with parity) exhibit even lower bit-error rates. The error rate for double scan without parity is less than  $10^{-11}$  for a signal-to-noise ratio of 4 db. The manufacturer makes no mention of the error rate for double scan with parity.

Under normal system operation, in which channel signal-to-noise ratio is greater than 12 dB and decoder double scan and parity tests are made upon received data, the likelihood of *all* released data being correct is essentially 100%.

#### D. Statistical Testing of Data Samples

The statistical test was set up as follows:

##### 1. Assumptions:

- Mean of sample means can be used as an estimate of population mean.<sup>4</sup>
- Population of differences is normal (Gaussian).

<sup>4</sup> Jerome C. R. Li, *Introduction to Statistical Inference*, pp. 33-35 (discussion of Central Limit Theorem and associated theorems concerning sample means). Published by Author, 1957.

2. Hypothesis: The population mean is equal to the mean of the sample means (10.6156), i.e., the difference between the two gauges is a constant.

Note: The difference between the gauges cannot be zero, even for perfect agreement, because:

a. there are differences in leveling between the two gauges (gauges do not have same zero).

b. an arbitrary amount (approx. 10 ft) is added to standard gauge readings to assure that all values are positive.

3. Level of significance: The 5% significance level was chosen. (This means the probability of rejecting a true hypothesis is 5%).

4. Statistic: The *t*-statistic was chosen because it tests a hypothesis on the population mean using the sample mean and sample standard deviation. (This choice is necessary here because the population standard deviation is not known.)

5. Critical regions: The critical regions for the *t*-statistic at the 5-percent level for a sample size of 24 are  $t < -2.069$  and  $t > 2.069$ . Values of *t* within these two intervals lead to rejection of the assumed hypothesis. Values of *t* outside the critical regions, i.e., within the interval  $-2.069 < t < +2.069$  lead to acceptance of the hypothesis. *t*-values calculated from 95 percent of all possible samples of size 24 will fall into this region. (Note that this does *not* mean 95% of the samples picked for analysis.)

6. *t*-values: The *t*-values for the four samples were calculated using the expression

$$t = \frac{\bar{y} - \mu_0}{\left(\frac{s^2}{n}\right)^{1/2}}$$

where  $\bar{y}$  = sample mean

$\mu_0$  = hypothetical population mean  
= 10.6156 in this analysis

$s^2$  = sample variance (square of sample standard deviation)

$n$  = sample size

The four *t*-values obtained were: 0.2188, -1.745 0.8085, 1.1739.

All four values are greater than -2.069 and less than +2.069, i.e., they are outside the critical regions. Thus, for the four samples considered, the hypothesis "population mean = 10.6156" was accepted at the 5-percent significance level.

Columns 6 and 7 of Table 1, and the section of the page below the table show the calculation of the *t*-statistic for one sample.

Table 1.—Data and statistical calculations for a representative sample

1 Time	2 Strip	3 Corr.	4 ADR	5 $y$	6 $(y - \bar{y})$	7 $(y - \bar{y})^2$
0100	3.70	3.79	14.41	10.62	.0017	$2.89 \times 10^{-6}$
0207	3.30	3.38	14.01	10.63	.0117	$136.89 \times 10^{-6}$
0321	3.40	3.48	14.10	10.62	.0017	$2.89 \times 10^{-6}$
0358	3.80	3.90	14.52	10.62	.0017	$2.89 \times 10^{-6}$
0501	4.70	4.82	15.43	10.61	.0083	$68.89 \times 10^{-6}$
0606	5.30	5.43	16.03	10.60	.0183	$334.89 \times 10^{-6}$
0656	5.50	5.64	16.24	10.60	.0183	$334.89 \times 10^{-6}$
0758	5.30	5.43	16.05	10.62	.0017	$2.89 \times 10^{-6}$
0858	4.90	5.02	15.65	10.63	.0117	$136.89 \times 10^{-6}$
0956	4.40	4.51	15.11	10.60	.0183	$334.89 \times 10^{-6}$
1102	3.80	3.90	14.52	10.62	.0017	$2.89 \times 10^{-6}$
1205	3.30	3.38	14.01	10.63	.0117	$136.89 \times 10^{-6}$
1318	3.00	3.08	13.69	10.61	.0083	$68.89 \times 10^{-6}$
1416	2.80	2.87	13.50	10.63	.0117	$136.89 \times 10^{-6}$
1534	2.90	2.97	13.59	10.62	.0017	$2.89 \times 10^{-6}$
1600	3.20	3.28	13.89	10.61	.0083	$68.89 \times 10^{-6}$
1700	4.20	4.30	14.92	10.62	.0017	$2.89 \times 10^{-6}$
1758	5.00	5.12	15.74	10.62	.0017	$2.89 \times 10^{-6}$
1903	5.60	5.74	16.38	10.64	.0217	$470.89 \times 10^{-6}$
1953	5.90	6.05	16.65	10.60	.0183	$334.89 \times 10^{-6}$
2106	5.70	5.84	16.47	10.63	.0117	$136.89 \times 10^{-6}$
2158	5.20	5.33	15.98	10.63	.0117	$136.89 \times 10^{-6}$
2306	4.40	4.51	15.12	10.61	.0083	$68.89 \times 10^{-6}$
2350	3.90	4.00	14.62	10.62	.0017	$2.89 \times 10^{-6}$

Key to columns

1 Time of readings

Sample variance

$$s^2 = \frac{\Sigma(y - \bar{y})^2}{n-1} = \frac{.00293336}{23}$$

2 Strip chart reading (ft.)

$$= 0.000127537$$

3 Strip chart reading, corrected for density

4 ADR reading from printout (ft.)

Sample standard deviation

$$s = 0.0112932$$

5 Difference (ADR minus corrected strip reading)

6 Difference (col. 5) minus average of differences

t-test

7 Square of quantity obtained in col. 6

$$H_0: \mu_0 = 10.6156$$

$$t = \frac{\bar{y} - \mu_0}{\sqrt{\frac{s^2}{n}}} = \frac{10.6183 - 10.6156}{\sqrt{\frac{0.0112932}{23}}} = \frac{0.0027}{\sqrt{0.000127537}} = \frac{0.0027}{0.0112932} = 0.238$$

Calculations

$$\bar{y}: 10.6183 \quad \Sigma(y - \bar{y})^2: 2933.36 \times 10^{-6}$$

$$t = 1.1738$$

NOAA TECHNICAL REPORTS

NOS 41 A User's Guide to a Computer Program for Harmonic Analysis of Data at Tidal Frequencies. R. E. Dennis and E. E. Long, July 1971. Price \$0.65 (COM-71-50606)

NOS 42 Computational Procedures for the Determination of a Simple Layer Model of the Geopotential From Doppler Observations. Bertold U. Witte, April 1971. Price \$0.65 (COM-71-50400)

NOS 43 Phase Correction for Sun-Reflecting Spherical Satellite. Erwin Schmid, August 1971. Price \$0.25 (COM-72-50080)

NOS 44 The Determination of Focal Mechanisms Using P- and S-Wave Data. William H. Dillinger, Allen J. Pope, and Samuel T. Harding, July 1971. Price \$0.60 (COM-71-50392)

NOS 45 Pacific SEAMAP 1961-70 Data for Area 15524-10: Longitude 155°W to 165°W, Latitude 24°N to 30°N, Bathymetry, Magnetics, and Gravity. J. J. Dowling, E. E. Chiburis, P. Dehlinger, and M. J. Yellin, January 1972. Price \$3.50 (COM-72-51029)

NOS 46 Pacific SEAMAP 1961-70 Data for Area 15530-10: Longitude 155°W to 165°W, Latitude 30°N to 36°N, Bathymetry, Magnetics, and Gravity. J. J. Dowling, E. F. Chiburis, P. Dehlinger, and M. J. Yellin, January 1972. Price \$3.50

NOS 47 Pacific SEAMAP 1961-70 Data for Area 15248-14: Longitude 152°W to 166°W, Latitude 48°N to 54°N, Bathymetry, Magnetics, and Gravity. J. J. Dowling, E. F. Chiburis, P. Dehlinger, and M. J. Yellin, April 1972. Price \$3.50 (COM-72-51030)

NOS 48 Pacific SEAMAP 1961-70 Data for Area 16648-14: Longitude 166°W to 180°, Latitude 48°N to 54°N, Bathymetry, Magnetics, and Gravity. J. J. Dowling, E. F. Chiburis, P. Dehlinger, and M. J. Yellin, April 1972. Price \$3.00 (COM-72-51028)

NOS 49 Pacific SEAMAP 1961-70 Data for Areas 16530-10 and 17530-10: Longitude 165°W to 180°, Latitude 30°N to 36°N, Bathymetry, Magnetics, and Gravity. E. F. Chiburis, J. J. Dowling, P. Dehlinger, and M. J. Yellin, July 1972. Price \$4.75

NOS 50 Pacific SEAMAP 1961-70 Data for Areas 16524-10 and 17524-10: Longitude 165°W to 180°, Latitude 24°N to 30°N, Bathymetry, Magnetics, and Gravity. E. F. Chiburis, J. J. Dowling, P. Dehlinger, and M. J. Yellin, July 1972. Price \$5.75

NOS 51 Pacific SEAMAP 1961-70 Data for Areas 15636-12, 15642-12, 16836-12, and 16842-12: Longitude 156°W to 180°, Latitude 36°N to 48°N, Bathymetry, Magnetics, and Gravity. E. F. Chiburis, J. J. Dowling, P. Dehlinger, and M. J. Yellin, July 1972. Price \$11.00 (COM-73-50280)

NOS 52 Pacific SEAMAP 1961-70 Data Evaluation Summary. P. Dehlinger, E. F. Chiburis, and J. J. Dowling, July 1972. Price \$0.40

NOS 53 Grid Calibration by Coordinate Transfer. Lawrence W. Fritz, November 1971. (COM-73-50240)

NOS 54 A Cross-Coupling Computer for the Oceanographer's Askania Gravity Meter. Carl A. Pearson and Thomas E. Brown, November 1972.

NOS 55 A Mathematical Model for the Simulation of a Photogrammetric Camera Using Stellar Control. Chester C. Slama, December 1972.

NOS 56 Cholesky Factorization and Matrix Inversion. Erwin Schmid, March 1973.

NOS 57 Complete Comparative Calibration. Lawrence W. Fritz, in press, 1973.